Contrib. Astron. Obs. Skalnaté Pleso **52/3**, 105 – 115, (2022)
https://doi.org/10.31577/caosp.2022.52.3.105

Monitoring solar activity during 23/24 solar cycle minimum through VLF radio signals

A. Kolarski, V.A. Srećković and Z.R. Mijić

Institute of Physics Belgrade, University of Belgrade, Pregrevica 118, 11080 Belgrade, Serbia (E-mail: aleksandra.kolarski@ipb.ac.rs)

Received: July 20, 2022; Accepted: October 2, 2022

Abstract. Solar activity during solar minimum between 23^{rd} and 24^{th} solar cycle was inspected, based on solar X-ray radiation listings from Geostationary Operational Environmental Satellite (GOES) database. Periods of quiet solar conditions with low background X radiation are particularly favourable for analysis and exploration of low intensity solar flare events and their effects on lower ionosphere. Low intensity solar flare events were monitored and examined through Very Low Frequency (VLF) radio signals (3-30 kHz), recorded by the use of Absolute Phase and Amplitude Logger system (AbsPAL) operating at the Institute of Physics Belgrade, Serbia. For the purposes of numerical modeling of low ionospheric response to low class solar flare events, the Long Wave Propagation Capability (LWPC) software, based on Wait's theory, was applied. Main results are presented in this paper.

Key words: Solar activity – Solar X-ray flares – radio signal perturbations

1. Introduction

During quiet solar conditions, ionization i.e. production of electron content within lower ionospheric D-region, within altitude range 50-90 km, is in general related to photoionization processes caused by UV Lyman-α spectral line 121.6 nm, EUV spectral lines ranging from 102.7 nm to 118.8 nm and galactic cosmic rays. One of frequent extraterrestrial causing agents, that become major source of electron density perturbations within D-region, are X-ray solar flare events (0.1-0.8 nm) (Whitten & Poppoff, 1965; Wang et al., 2020; Hayes et al., 2021). Due to additional ionization, electron density height profile of the lower ionosphere changes (Mitra, 1974). Such perturbations affect propagation of Very Low Frequency (VLF) radio signals within Earth-ionosphere waveguide, causing deviations from their regular propagation patterns stable at unperturbed solar conditions (Thomson, 1993; McRae & Thomson, 2000). Since electron production rate coefficients can be considered directly proportional to intensity of incident X-radiation (Ratcliffe et al., 1972), perturbations of VLF radio signals induced by solar flares can be used as diagnostic tool for exploration of lower ionospheric electron content behavior during such events (see Barta et al., 2022, and references therein).

Utilization of VLF radio signals, as the remotesensing technique for exploration of the lower ionosphere (Thomson et al., 2011; McRae & Thomson, 2000; McRae & Thomson, 2004; Thomson et al., 2005), is widely adopted and extensively used by many research groups over several decades, e.g. (Silber & Price, 2017) and references therein. Response of the lower ionosphere to analyzed solar flare events, numerically was modeled by the use of Long Wave Propagation Capability (LWPC) (Ferguson, 1998) software relying on application of Wait's theory (Wait & Spies, 1964).

Effects of low intensity solar flare events of C and B classes, during 23/24 solar minimum, between descending branch of 23^{rd} and ascending branch of 24^{th} solar cycle, were inspected by monitoring recordings of VLF radio signals recorded in Belgrade (44.85 N, 20.38 W) Serbia, within time period from 2008 to 2010. Data related to solar X-rays is obtained from Geostationary Operational Environmental Satellite (GOES) archive database (`https://satdat.ngdc.noaa.gov/sem/goes/data/avg/`).

2. Observations

Periods of quiet solar activity, like during solar minimums, are of great interest for studying quiet ionospheric conditions and accompanying quiet i.e. unperturbed states within Earth-ionosphere waveguide related to VLF radio signals' transmission. In addition, since solar background X radiation during such periods is of small amount, low class solar flare events, like those of lower C class and moderate B class, when occur, are easily noticeable and recognizable, clearly distinguishing themselves from surrounding sections of unperturbed VLF radio signals. This gives a unique opportunity to examine characteristics of low class solar flare events, which are otherwise masked by high solar background X radiation during periods of usual more intense solar activity. An example of active Sun during solar maximum in April 2014 and quiet Sun during solar minimum in December 2019 are given in Figure 1, left and right, respectively. In 23/24 solar minimum, during 2008 there were 8 C class and 1 M class solar flare events reported, with X-ray background flux up to A8.1, while during 2009 there were 28 C class solar flare events reported, with X-ray background flux up to B1.4 (Figure 2).

VLF radio signal recordings obtained from the Absolute Phase and Amplitude Logger receiving station (AbsPAL), located and operating at the Institute of Physics in Belgrade, Serbia, was used as instrumental setup. Within inspected time period from 2008 to 2010, several VLF radio signals were simultaneously recorded by AbsPAL station in Belgrade. Geographical position and transmitter's characteristics of VLF radio signals propagating towards Belgrade are given in Table 1.

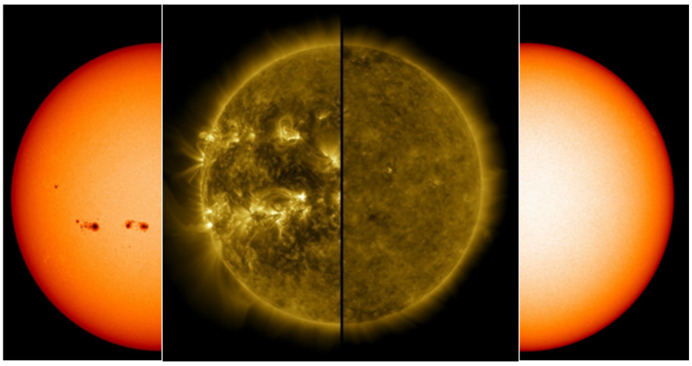

Figure 1. Active Sun during solar max. in April 2014 (left) and quiet Sun during solar min. in December 2019 (right) (taken from https://www.nasa.gov/).

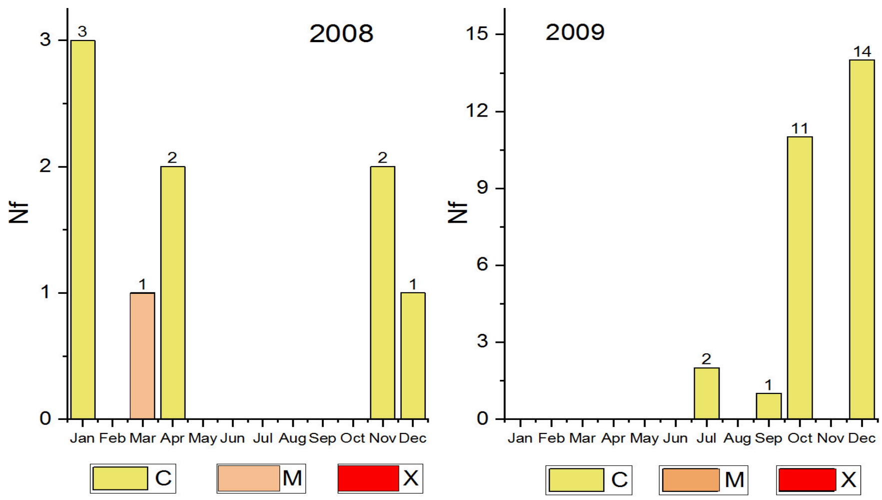

Figure 2. Solar flare events reported in period 2008-2010.

3. Results and discussion

Inspection of low intensity solar flare events of C and B class, on recorded VLF radio signals, was done according to provided solar X radiation listings from GOES database. During inspected period 2008-2010, low class solar flare events exhibited expected behavior, with amplitude perturbations of absolute amount in general of several tenth parts of dB up to few dB and with phase delay perturbations of absolute amount of few degrees to up to 16^{o}. Some typical

Table 1. VLF radio signals registered in Belgrade during 23/24 solar cycle minimum.

VLF signal (kHz)	Transmitter	Broadcast Power (kW)	GCP* Distance (km)
GQD/22.1	Skelton, UK (54.72N; 2.88W)	500	1982
NAA/24.0	Maine, USA (44.63N; 67.28W)	1000	6547
NWC/19.8	H. E. Holt, Australia (27.2S; 114.98E)	1000	11975
DHO/23.4	Rhauderfehn, Germany (53.08N; 7.62E)	800	1301
ICV/20.27	Isola di Tavolara, Italy (NATO) (40.92N; 9.73E)	20	970
HWU/18.3	Rosnay, France (NATO) (46.71N; 1.24E)	400	1493

*Great Circle Path (GCP)

examples of low intensity solar flare events and accompanied VLF radio signal perturbations registered in Belgrade are given in Figures 3-4. However, in some cases, relatively weak solar flare events induced amplitude perturbations of as much as 5 dB and 13°, while from relatively stronger ones, perturbations reached as much as 5 dB and 15° (Figures 5-8). Particularly interesting case was solar flare event of B class B8.35 which induced amplitude perturbation in NAA/24.0 kHz radio signal of 1.5 dB and phase delay perturbation of 10° (Figures 9-10, rounded by oval and enlarged in Figures 11-12).

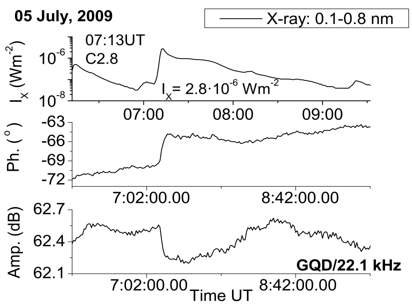

Figure 3. GQD signal perturbation during C2.8 class X-ray solar flare event.

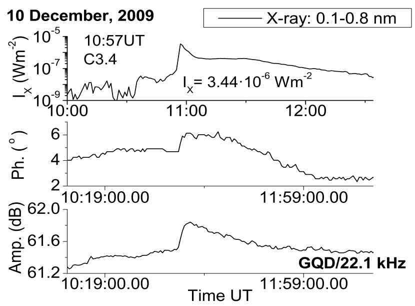

Figure 4. GQD signal perturbation during C3.4 class X-ray solar flare event.

Electron density height profile within Earth's lower ionosphere changes due to the incident solar X-ray radiation during solar flare events, causing in general descending and "sharpening" of the ionospheric lower boundary. Model of VLF radio signals propagation within Earth-ionosphere waveguide (Wait & Spies, 1964), that describes the electron density by reflecting edge sharpness,

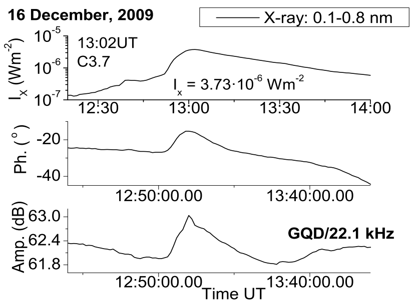

Figure 5. GQD signal perturbation during C3.7 class X-ray solar flare event.

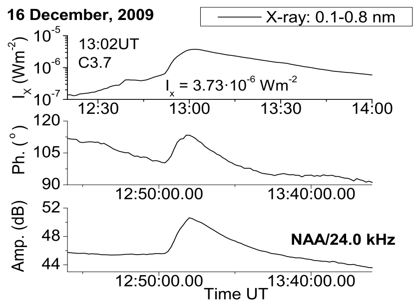

Figure 6. NAA signal perturbation during C3.7 class X-ray solar flare event.

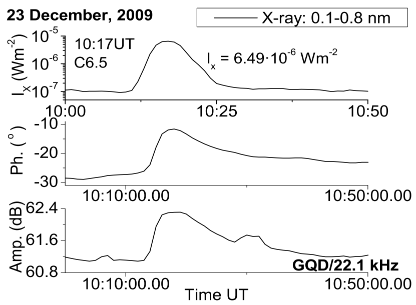

Figure 7. GQD signal perturbation during C6.5 class X-ray solar flare event.

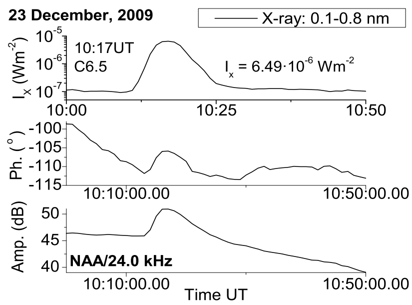

Figure 8. NAA signal perturbation during C6.5 class X-ray solar flare event.

denoted by β (km^{-1}) and reflecting edge height, denoted by H' (km), was used for purposes of numerical simulations of VLF radio signal propagation through Earth-ionosphere waveguide. Obtained results through simulations are in good agreement with VLF signal amplitude and phase delay data measured in Belgrade. Electron density height profiles N_e(z), within altitude range 50-90 km, were obtained through the equation (Wait & Spies, 1964):

$$N_e(z, H', \beta) = 1.43 \cdot 10^{13} e^{-0.15H'} e^{(\beta-0.15)(z-H')} \, . \tag{1}$$

Numerical simulations were conducted for the entire time evolution of chosen solar flare events, with parameter pairs (β/H') held constant along VLF radio signal's GCPs, depicting "average" ionospheric conditions within waveguide. VLF radio signal's amplitude and phase delay perturbations ΔA (dB) and ΔP (°), were determined by comparing measured perturbed to the measured

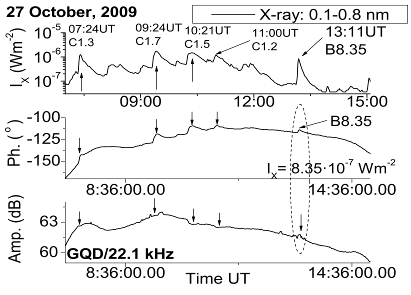

Figure 9. GQD signal perturbations during October 27^{th}, 2009.

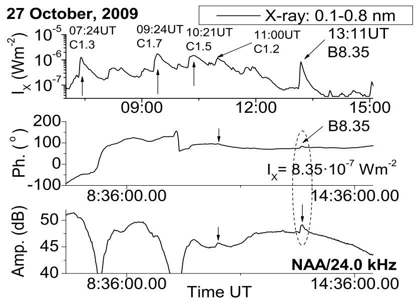

Figure 10. NAA signal perturbations during October 27^{th}, 2009.

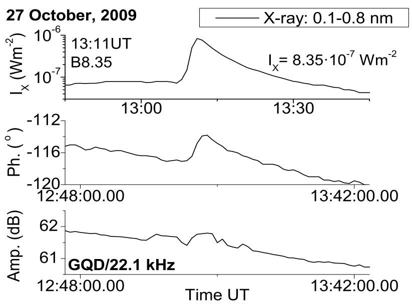

Figure 11. GQD signal perturbation during B8.35 class X-ray solar flare event.

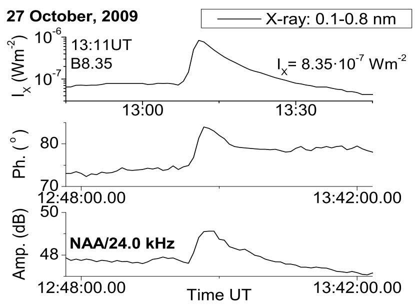

Figure 12. NAA signal perturbation during B8.35 class X-ray solar flare event.

unperturbed amplitude and phase delay values and are calculated as: $\Delta A = A_{flare}$ - A_{unpert} and $\Delta P = P_{flare}$ - P_{unpert}. During simulations through iterative process, the goal was to achieve as close as possible to measured data, both absolute values of simulated amplitude and phase delay and relative amount of perturbations. Results obtained through numerical simulations are in good agreements with measured data. Calculated electron density height profiles during maximum of X-ray solar irradiance, in case of NAA/24.0 kHz signal trace, are given in (Figure 13), for some chosen examples of solar flare events: a) low intensity C class solar flare event C3.7 that occurred on December 16^{th}, 2009, at 13:02UT with $I_{max} = 3.73 \cdot 10^{-6}$ Wm^{-2}, with measured ΔA_{flare}=5 dB and ΔP_{flare}=13° and through simulations obtained parameter pair (β/H') (0.43 km^{-1}/69.7 km) with calculated electron density N_e(74 km)=1.37·10^9 m^{-3}, b) moderate intensity C class solar flare event C6.5 that occurred on December

23^{rd}, 2009, at 10:17UT with $I_{max} = 6.49{\cdot}10^{-6}$ Wm^{-2} with measured ΔA_{flare}=5 dB and ΔP_{flare}=6^{o} and through simulations obtained parameter pair (β/H') (0.43 km^{-1}/70.1 km) with calculated electron density N_e(74 km)=1.17$\cdot$10^9 m^{-3} and c) moderate intensity B class solar flare event B8.35 that occurred on October 27^{th}, 2009, at 13:11UT with $I_{max} = 8.35 \cdot 10^{-7}$ Wm^{-2} with measured ΔA_{flare}=1.5 dB and ΔP_{flare}=10^{o} and through simulations obtained parameter pair (β/H') (0.33 km^{-1}/72.3 km) with calculated electron density N_e(74 km)=3.79$\cdot$10^8 m^{-3}. Obtained electron density height profiles in flare state, with N_e(74 km) increase of about one order of magnitude in case of C class flares, with slight increase of about 75% in case of B class flare, are realistic and in line with other studies (Žigman et al., 2007; Grubor et al., 2008; McRae & Thomson, 2004; Kolarski et al., 2011; Nina et al., 2011, 2012; Kolarski & Grubor, 2014; Kolarski et al., 2022; Srećković et al., 2021a,b).

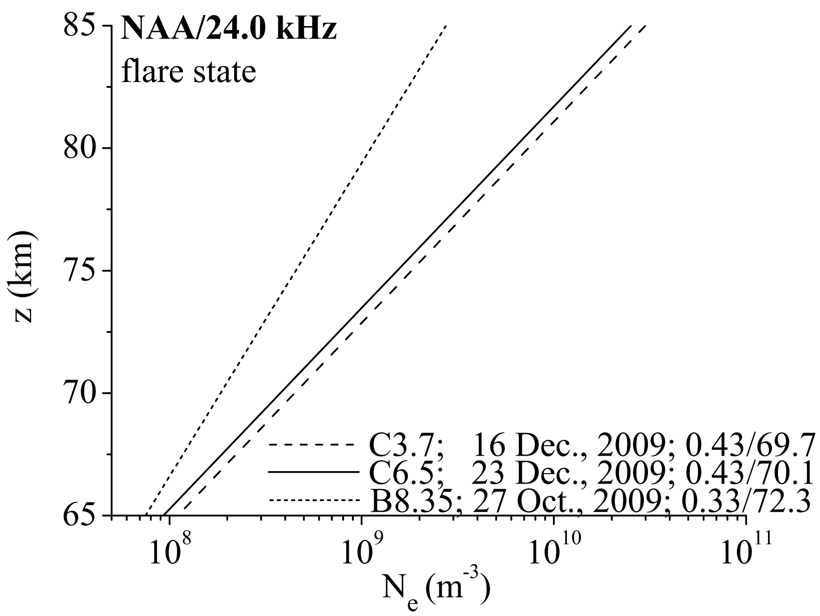

Figure 13. Electron density height profiles during C3.7 (dashed line), C6.5 (solid line) and B8.35 (dotted line) class X-ray solar flare events.

It is possible to draw conclusions about the intensity of the causing X-ray solar flare events, based upon perturbation amounts obtained from VLF radio signal recordings, when taking into consideration single VLF radio signal trace.

However, same solar flare event can produce perturbations different both in pattern and in intensity, when observed on different VLF radio signal traces. Typical examples are in general perturbations induced by solar flare events of moderate and lower intensity classes as recorded in Belgrade during active solar periods on NAA and GQD radio signals. In such cases, NAA signal's both amplitude and phase delay follow in pattern incident X-ray solar irradiance, while in case of GQD signal, amplitude and phase delay follow incident X-ray solar irradiance in pattern, but like mirrored images and only in some cases of higher class solar flare events this feature is more or less mitigated (Žigman et al., 2007; Grubor et al., 2008; Kolarski & Grubor, 2014). Aside to main factor of solar flare intensity (Grubor et al., 2008; Kolarski & Grubor, 2014), this behavior is also strongly under the influence of VLF GCP trace characteristics (Kolarski & Grubor, 2015; Šulić & Srećković, 2014; Šulić et al., 2016). For example, measured absolute perturbation as observed on GQD radio signal trace, in case of C3.7 solar flare event was ΔA_{flare}=1 dB and ΔP_{flare}=11.5^o, in case of C6.5 solar flare event was ΔA_{flare}=1.2 dB and ΔP_{flare}=15.5^o and in case of B8.35 solar flare event it was ΔA_{flare}=0.4 dB and ΔP_{flare}=3.3^o.

4. Summary

Two year time period of VLF radio signal recordings from Belgrade AbsPAL database, corresponding to 23/24 solar minimum, was examined in order of getting better insight of effects that low intensity solar flare events of C and B classes have on the lower ionospheric region and transmission of VLF radio signals within Earth-ionosphere waveguide. According to GOES database, during inspected period 2008-2010, 38 solar flare events of C and M class were reported, with X-ray background flux in range up to A8.1 for 2008 and B1.4 for 2009. Low intensity solar flare events of C and B class were monitored on all recorded VLF radio signals. Depending on solar flare occurrence time and VLF radio signal's GCP towards Belgrade receiver station, some flares were simultaneously observed on several VLF radio signals, however, detailed analysis in this paper was conducted for cases of NAA/24.0 kHz and GQD/22.1 kHz signal traces.

As expected, majority of low class solar flare events in general revealed perturbations of absolute amount of several tenth parts of dB up to few dB and of few degrees to up to 16^o, following the manner of incident solar X-ray flux. However, there were also cases that fall out of the pattern, when relatively weak solar flare events such as C3.7, produced perturbations of 5 dB and 13^o, while relatively stronger ones, such C6.5 gave perturbations of similar amount, as 5 dB and 15^o. Due to low X-ray background flux, in some cases even B class solar flare events induced noticeable perturbations, as in case of B8.35 with perturbation of 1.5 dB and 10^o.

Numerical simulations were conducted using LWPC software package, with goal of achieving simulated VLF data as close as possible to measured VLF data in Belgrade, both in case of absolute values and in case of relative amount of perturbations. Results obtained through iterative numerical simulations are in good agreements with real VLF data measured in Belgrade (Žigman et al., 2007; Grubor et al., 2008; Kolarski et al., 2011; Nina et al., 2011). In case of NAA/24.0 kHz signal, perturbations induced by low class solar flare events produced "sharpening" and descending of the lower ionospheric boundary, as in cases of presented solar flare events reflection height went from unperturbed value of 74 km to 72.3, 70.1 and 69.7 km, while become "sharper" compared to unperturbed value of 0.3 km^{-1} reaching 0.33 and 0.44 km^{-1}. Estimated N_e(74 km) are realistic and in line with other studies (McRae & Thomson, 2004; Nina et al., 2012; Kolarski & Grubor, 2014; Kolarski et al., 2022; Srećković et al., 2021a,b).

Acknowledgements. Authors thank D. Šulić for instrumental setup. This work was funded by the Institute of Physics Belgrade through a grant by the Ministry of Education, Science, and Technological Development of the Republic of Serbia. Authors appreciate comments expressed by referees, which improved this paper.

References

Barta, V., Natras, R., Srekovi, V., et al., Multi-instrumental investigation of the solar flares impact on the ionosphere on 0506 December 2006. 2022, *Frontiers in Environmental Science*, **10**, DOI: 10.3389/fenvs.2022.904335

Ferguson, J. 1998, Computer programs for assessment of long-wavelength radio communications, version 2.0: User's guide and source files, Tech. rep., Space and naval warfare systems center San Diego CA

Grubor, D., Šulić, D., & Žigman, V., Classification of X-ray solar flares regarding their effects on the lower ionosphere electron density profile. 2008, *Annales Geophysicae*, **26**, 1731, DOI: 10.5194/angeo-26-1731-2008

Hayes, L. A., O'Hara, O. S. D., Murray, S. A., & Gallagher, P. T., Solar Flare Effects on the Earth's Lower Ionosphere. 2021, *Solar Physics*, **296**, 157, DOI: 10.1007/s11207-021-01898-y

Kolarski, A. & Grubor, D., Sensing the Earths low ionosphere during solar flares using VLF signals and goes solar X-ray data. 2014, *Advances in space research*, **53**, 1595, DOI: 10.1016/j.asr.2014.02.022

Kolarski, A. & Grubor, D., Comparative analysis of VLF signal variation along trajectory induced by X-ray solar flares. 2015, *Journal of Astrophysics and Astronomy*, **36**, 565, DOI: 10.1007/s12036-015-9361-x

Kolarski, A., Grubor, D., & Šulić, D., Diagnostics of the Solar X-Flare Impact on Lower Ionosphere through the VLF-NAA Signal Recordings. 2011, *Open Astronomy*, **20**, 591, DOI: 10.1515/astro-2017-0342

Kolarski, A., Srećković, V. A., & Mijić, Z. R., Response of the Earths Lower Ionosphere to Solar Flares and Lightning-Induced Electron Precipitation Events by Analysis of VLF Signals: Similarities and Differences. 2022, *Applied Sciences*, **12**, 582, DOI: 10.3390/app12020582

McRae, W. M. & Thomson, N. R., VLF phase and amplitude: Daytime ionospheric parameters. 2000, *Journal of Atmospheric and Solar-Terrestrial Physics*, **62**, 609, DOI: 10.1016/S1364-6826(00)00027-4

McRae, W. M. & Thomson, N. R., Solar flare induced ionospheric D-region enhancements from VLF phase and amplitude observations. 2004, *Journal of Atmospheric and Solar-Terrestrial Physics*, **66**, 77, DOI: 10.1016/j.jastp.2003.09.009

Mitra, A. P. 1974, *Ionospheric effects of solar flares* (Springer, Berlin/Heidelberg)

Nina, A., Čadež, V., Srećković, V., & Šulić, D., The influence of solar spectral lines on electron concentration in terrestrial ionosphere. 2011, *Open Astronomy*, **20**, 609, DOI: 10.1515/astro-2017-0346

Nina, A., Čadež, V., Srećković, V., & Šulić, D., Altitude distribution of electron concentration in ionospheric D-region in presence of time-varying solar radiation flux. 2012, *Nuclear Instruments and Methods in Physics Research Section B: Beam Interactions with Materials and Atoms*, **279**, 110, DOI: 10.1016/j.nimb.2011.10.019

Ratcliffe, J. A. et al. 1972, *An introduction to ionosphere and magnetosphere* (CUP Archive, Cambridge, UK)

Silber, I. & Price, C., On the use of VLF narrowband measurements to study the lower ionosphere and the mesosphere–lower thermosphere. 2017, *Surveys in Geophysics*, **38**, 407, DOI: 10.1007/s10712-016-9396-9

Srećković, V. A., Šulić, D. M., Ignjatović, L., & Vujčić, V., Low Ionosphere under Influence of Strong Solar Radiation: Diagnostics and Modeling. 2021a, *Applied Sciences*, **11**, 7194, DOI: 10.3390/app11167194

Srećković, V. A., Šulić, D. M., Vujčić, V., Mijić, Z. R., & Ignjatović, L. M., Novel Modelling Approach for Obtaining the Parameters of Low Ionosphere under Extreme Radiation in X-Spectral Range. 2021b, *Applied Sciences*, **11**, 11574, DOI: 10.3390/app112311574

Thomson, N., Experimental daytime VLF ionospheric parameters. 1993, *Journal of Atmospheric and Terrestrial Physics*, **55**, 173, DOI: 10.1016/0021-9169(93)90122-F

Thomson, N. R., Rodger, C. J., & Clilverd, M. A., Large solar flares and their ionospheric D region enhancements. 2005, *Journal of Geophysical Research: Space Physics*, **110**, DOI: https://doi.org/10.1029/2005JA011008

Thomson, N. R., Rodger, C. J., & Clilverd, M. A., Daytime D region parameters from long-path VLF phase and amplitude. 2011, *Journal of Geophysical Research: Space Physics*, **116**, DOI: https://doi.org/10.1029/2011JA016910

Šulić, D. M. & Srećković, V. A., A Comparative Study of Measured Amplitude and Phase Perturbations of VLF and LF Radio Signals Induced by Solar Flares. 2014, *Serbian Astronomical Journal*, **188**, 45, DOI: 10.2298/SAJ1488045S

Šulić, D. M., Srećković, V. A., & Mihajlov, A. A., A study of VLF signals variations associated with the changes of ionization level in the D-region in consequence of solar conditions. 2016, *Advances in Space Research*, **57**, 1029, DOI: 10.1016/j.asr.2015.12.025

Wait, J. R. & Spies, K. P. 1964, *Characteristics of the Earth-ionosphere waveguide for VLF radio waves* (US Department of Commerce, National Bureau of Standards, Boulder, CO, USA)

Wang, X., Chen, Y., Toth, G., et al., Predicting Solar Flares with Machine Learning: Investigating Solar Cycle Dependence. 2020, *Astrophysical Journal*, **895**, 3, DOI: 10.3847/1538-4357/ab89ac

Whitten, R. & Poppoff, I. 1965, *Physics of the Lower Ionosphere* (Prentice-Hall, Englewood Cliffs, N. J.)

Žigman, V., Grubor, D., & Šulić, D., D-region electron density evaluated from VLF amplitude time delay during X-ray solar flares. 2007, *Journal of atmospheric and solar-terrestrial physics*, **69**, 775, DOI: 10.1016/j.jastp.2007.01.012